S33-37
116735
26 P.

1987

NASA ASEE SUMMER FACULTY RESEARCH FELLOWSHIP PROGRAM

MARSHALL SPACE FLIGHT CENTER

THE UNIVERSITY OF ALABAMA HUNTSVILLE

Examination of the Physical Processes Associated With the
Keyhole Region of Variable Polarity Plasma Arc Welds in
Aluminum Alloy 2219

Prepared By: Daniel W. Walsh Ph.D.

Academic Rank: Associate Professor

University and Department: California Polytechnic State
                                    University, San Luis Obispo
                                    Metallurgy and Materials Eng

NASA/MSFC

Laboratory: Materials and Processes

Division: Process Engineering

Branch: Metals Processes

NASA Colleague: Arthur C. Nunes Jr., Ph.D.

Date: August 31, 1987

Contract Number:

ABSTRACT

The morphology and properties of the Variable Polarity Plasma Arc (VPPA) weld composite zone are intimately related to the physical processes associated with the keyhole. This study examined the effects of oxide, halide, and sulfate additions to the weld plate on the keyhole and the weld pool. Changes in both the arc plasma character and the bead morphology were correlated to the chemical environment of the weld. Pool behavior was observed by adding flow markers to actual VPPA welds. A low temperature analog to the welding process was developed. The results of the study indicate that oxygen, even at low partial pressures, can disrupt the stable keyhole and weld pool. The results also indicate that Marangoni surface tension driven flows dominate the weld pool over the range of welding currents studied.

Acknowledgement

Introduction

The physics associated with VPPA process is interesting for three reasons. First, the keyhole and pool are not well understood. In fact the VPPA keyhole process has not been as well characterized as either of the two high energy density beam keyhole processes, laser and electron beam. Second, fluid flow and heat transfer fix the distribution of microstructure and properties in the weld composite region. Finally, fluid flow in the pool and static forces on the pool determine weld bead morphology. The steady state keyhole, is shown in Figure 1. Energy is transferred to the work via a heated plasma directed by the plasma torch. The transfer process has been studied (1-4), and is quite different from other arc processes including the GTA process. Much of the energy transfer is accomplished by convective mechanisms in the hot, directed efflux plasma and by radiation from an arc that is buried in the keyhole region. In VPPA welding the arc polarity switches many times a second, but the work is principally anodic. The oxide film associated with Al 2219 is disrupted by the sputtering action of argon ions during the reverse polarity portion of the cycle, and the arc is stabilized. A majority of the heat transfer occurs at the leading edge of the keyhole, where the anode spot is located and the plasma is directed. In this location the liquid is thin and the thickness uniform regardless of depth in the keyhole (<0.5mm). Around the keyhole, until the longitudinal centerline is passed, the fluid remains thin, but the thickness is not as uniform, becoming slightly larger deeper in the keyhole. At the keyhole rear, a large croissant shaped fluid pool exists.

Several forces determine shape of the trailing pool: surface tension, weight, stagnation pressure of incident gas, and forces arising from flows in the fluid. Several authors have attempted to predict droplet shape, a priori, from a consideration of these forces. Most of these efforts treated fluids in situations less complex than that found in a weld pool(5,6). Heat transfer and pool flow are critical in determining pool and nugget shape. Many investigators have sought to relate penetration to flow in the weld pool. Several (7) postulated that electromagnetic (Lorentz) forces in the weld pool controlled flow. The Lorentz force is given by $\vec{f} = \vec{j} \times \vec{B}$, where j is the current density and B is the magnetic field strength. The force is directly proportional to current density and to magnetic field strength. These authors demonstrated parabolic relations between flow velocities and current in mercury baths, Figure 2. Further, the authors demonstrated an inverse relation
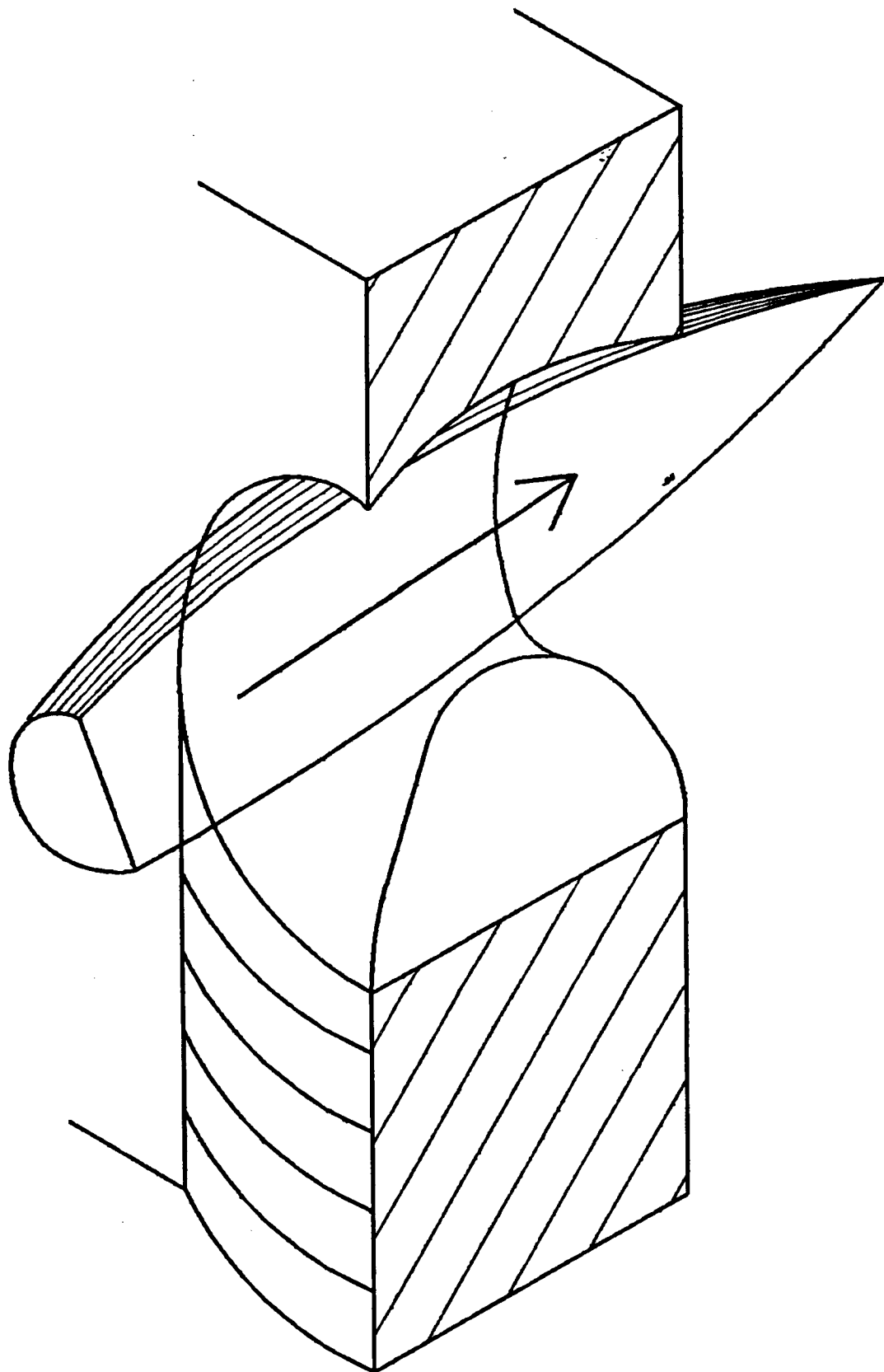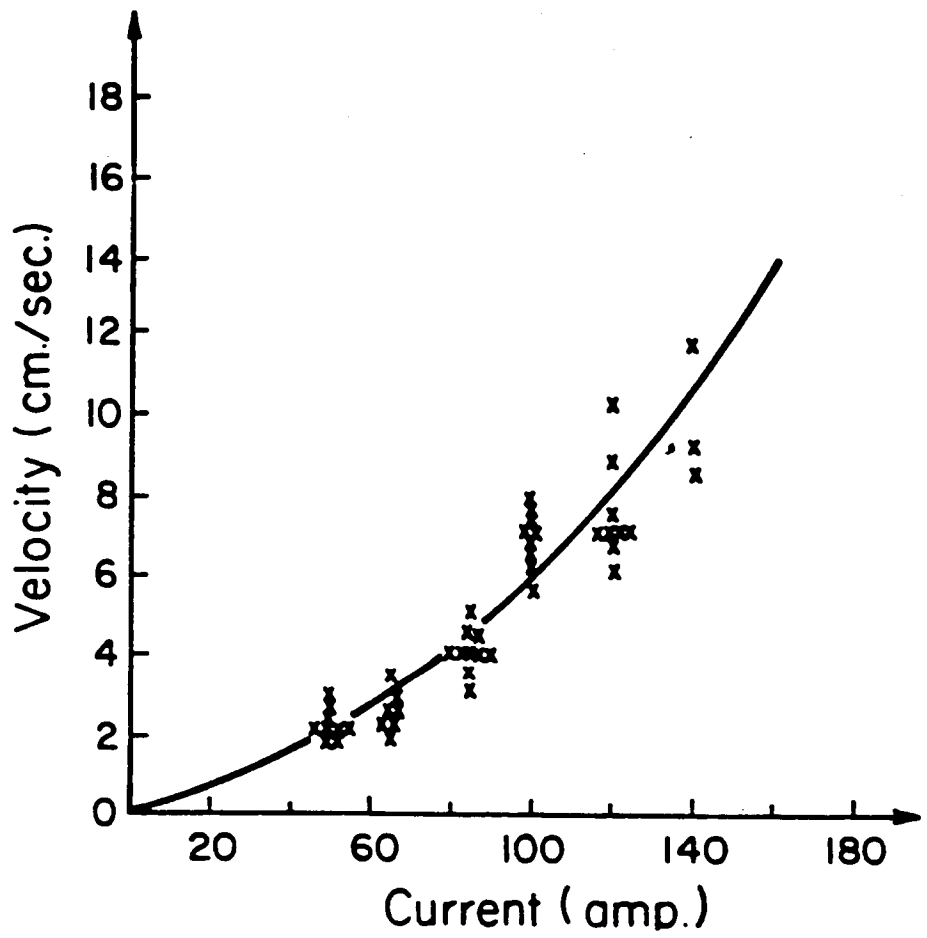
Figure 1 - Plasma Keyhole

XXXIV-2

Figure 3 - Flow of Mercury Driven by Lorentz Forces

XXXIV-3

between the velocity of flow and the electrode diameter. Lorentz forces promoted the establishment of downward flows under the arc supported by radially inward flows on the surface.

Surface-tension driven flows arise in welding systems because a surface-tension gradient exists on the pool surface. Material flows from regions of low surface tension to regions of high surface tension. The arc on the surface of the pool provides a radial thermal gradient, with higher temperatures in the regions directly beneath the arc. Many have modeled the pool surface temperature distribution and some have determined it experimentally. The temperature decays to the effective liquidus temperature at the pool boundary. Because surface tension is a strong function of temperature, a surface tension gradient is induced by the presence of an arc. The flow direction will depend strongly on the sign of the temperature coefficient of surface tension. Deep penetration is associated with those systems that have a positive coefficient (promoting inward flow). In this case the hottest fluid directly under the arc will be channeled downward to the base of the pool. Conversely, if the coefficient is negative, outward flow results and the hot metal erodes the edge of the pool increasing pool width, Figure 3. Elements that are not surface active themselves can have a profound effect on the pool flow by interacting with the surfactants.

The question of the heirarchy of flows in the weld pool can be addressed based on the work of several authors. Andrews and Craine,(8) and Atthey (9) discussed Lorentz induced flows in weld pools, generated by a distributed source of current. These authors predict flows that agree well with the empirical data. Mills (10) examined buoyancy, natural convection, as a source of pool flow. The ratio of thermal stirring to Lorentz stirring is less than 0.05 for values typical of welding arcs at less than 250 amperes. Furthermore, the Peclet number a ratio of heat transferred by convection to that transferred by conduction , falls in the range of 10 to 70 for weld pools. This indicates that convective heat transfer totally dominates in the pool, even when only Lorentz forces are considered.

Landau and Lifshitz (11) and Levich (12) have derived expressions for the surface velocity developed by a surface tension gradient: $Vel = \left(h/4\nu \right)\left(\partial\sigma/\partial T \right)\left(\partial T/\partial x \right)$
Where $\partial\sigma/\partial\sigma$ and $\partial T/\partial x$ are the surface tension and thermal gradients respectively, h is L, and ν is the kinematic viscosity. The substitution of conservative values for the parameters in this expression leads to the astounding conclusion that
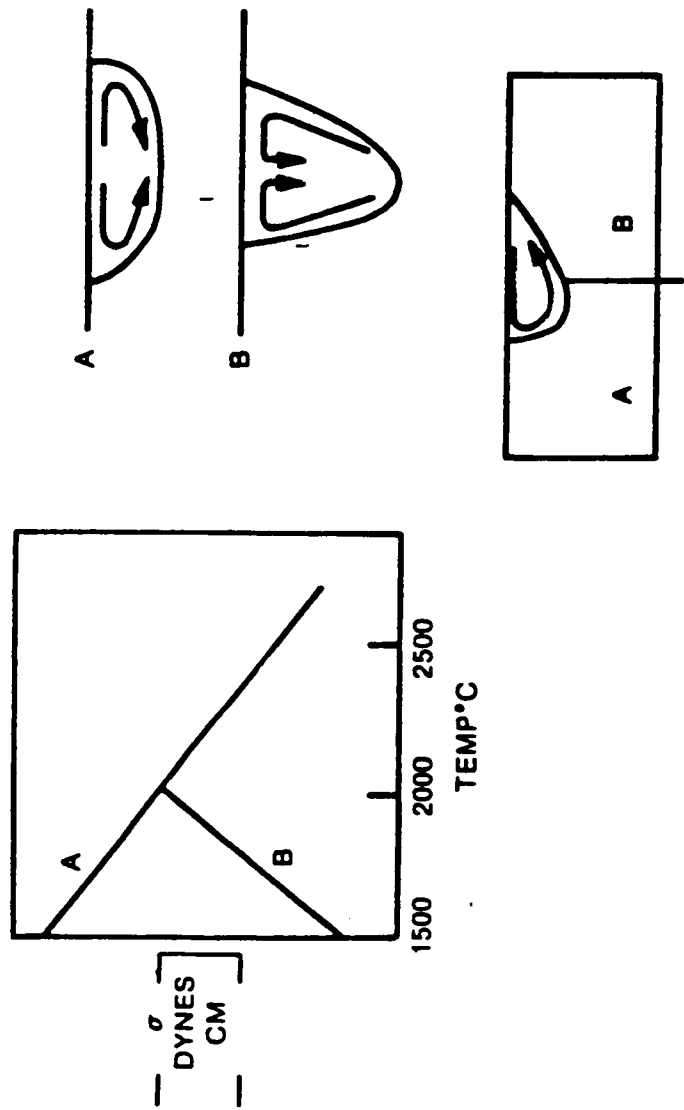
Figure 4 - Marangoni Flow in Weld Pools

XXXIV-5

surface-tension-driven flows develop a velocity of 50 to 150 cm/sec. This flow exists whether or not surface active species are present, only the direction of flow is affected by the fluid constitution. Kou (13) and Oreper (14) have developed computer codes to generate the predicted shape of stationary arc welds, both show that the surface-tension forces and the Lorentz forces dominate.

In conclusion, computations show that surface tension driven flows are dominant in the weld pool. Further, convective transfer in the pool is fifty times more efficient than conduction. The forces on the weld pool, at currents up to 250 amperes, produce velocities up to the following magnitudes; buoyancy, 0.5 cm/sec; Lorentz, 10.0 cm/sec; Marangoni 125 cm/sec. The flow generated by each of these mechanisms is depicted in Figure 4. The Lorentz force is expected to be even less significant in the case of VPPA welds because it acts on a very thin liquid layer at the leading edge of the keyhole. Even though the polarity, and thus the magnetic fields, change rapidly the Lorentz force will act consistently because the current density vector reverses with the magnetic field.

Figure 5 is a photograph of the rear keyhole of a VPPA weld on Al 2219. The backside appearance supports the contention that direct Marangoni flow dominates the pool. The weld bead is set off by two parallel rectangles that extend along its entire length. These are regions where a tightly adherent oxide skin has served to retain a fully fluid region beneath. In the peaked central region of the reinforcement a corrugated, heavily oxidized surface is evident. The appearance is derived from the "ice jam" of oxide residues freed up on the front side by cathodic cleaning and carried to the backside by the convergence of vigorous Marangoni flows.
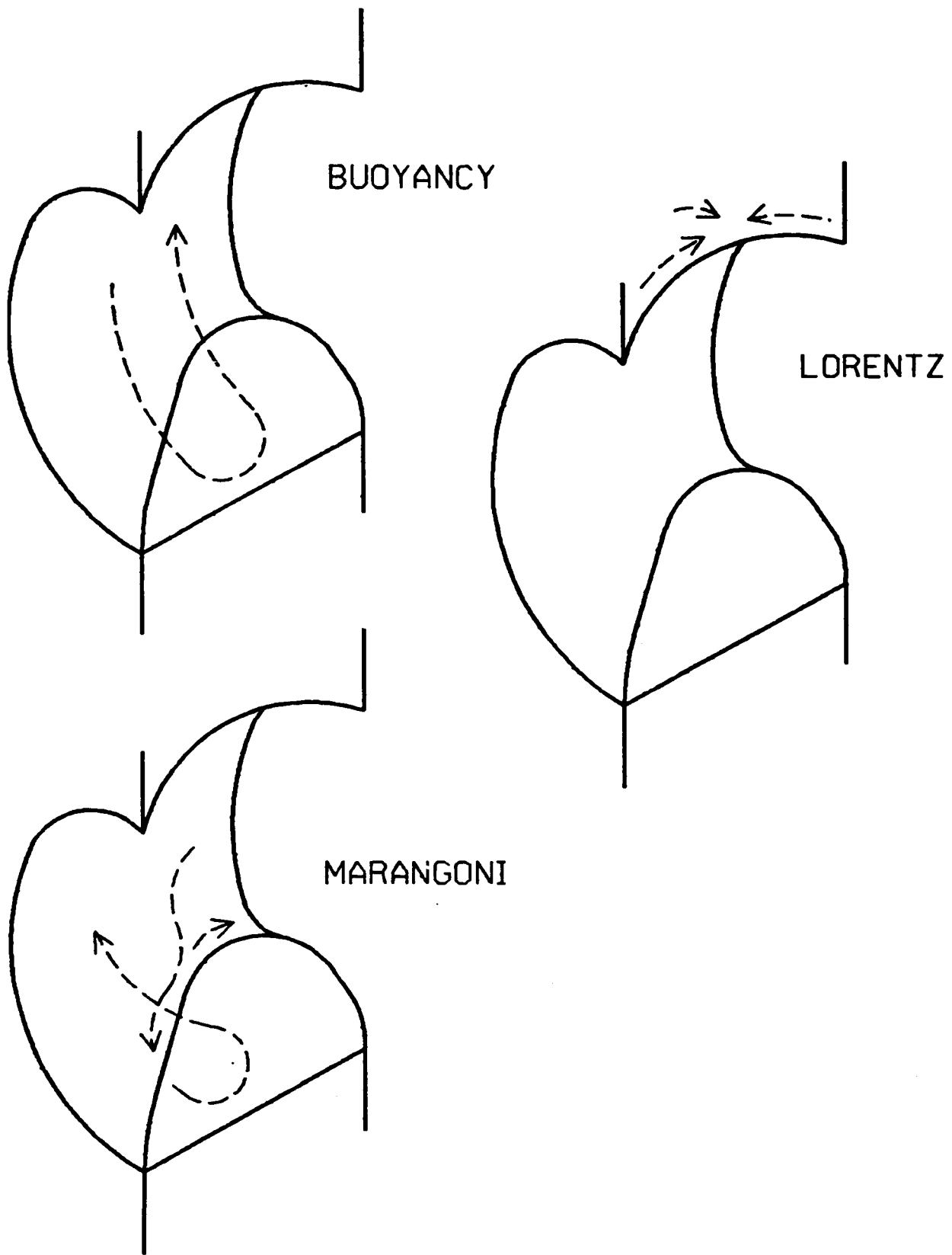
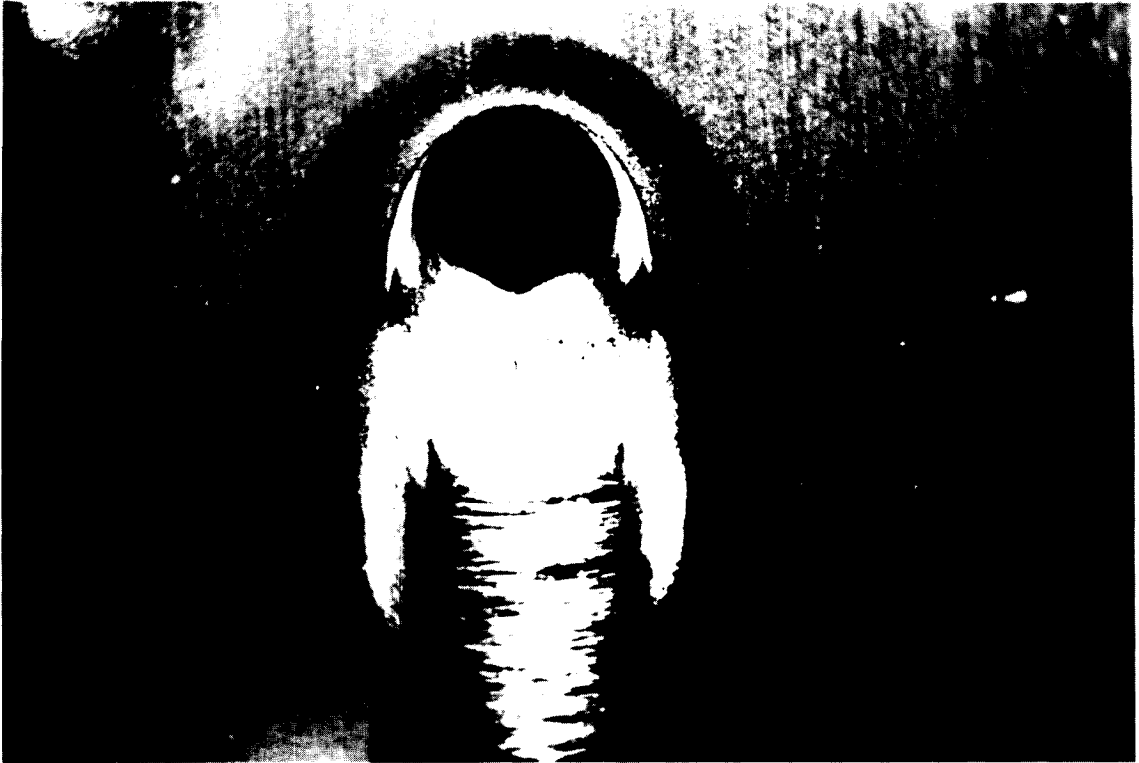Figure 5 - Flow in Plasma Keyholes

XXXIV-7

Figure 5. Rear Side, Actual Keyhole.

Materials and Procedures

The experimental portion of this study is comprised of three major programs:
  (1) Determination of the effects of chemical additions on weld bead shape and keyhole morphology.
  (2) Determination of the flow in regions surrounding the keyhole using a marker technique.
  (3) Development of an easily studied analog to fluid flow in the keyhole regions of VPPA welds in Aluminum 2219 T87. (Al 2219)

In the first program a series of 0.375 inch thick Al 2219 plates were treated with chemicals prior to welding. After the entire plate was thouroughly cleaned with solvent, a small region (2" by 4") was coated with the chemical agent of interest. The chemicals were placed on the plate surface as water based slurries or saturated aqueous solutions. The amount of chemical deposited on the surface was estimated as 0.02 to 0.20 grams (200 to 2000 parts per million).

Each plate was welded in the vertical position, employing a welding schedule developed for production welds in plates of this thickness. When stable, steady state welding conditions were attained, the welding head standoff was fixed rigidly. In order to attain the steady state condition, a total weld length of fourteen inches was used, only the final four inches of each weld was altered by chemical addition. All welding parameters were recorded during the test, the readings were taken at two second intervals. The posterior of the keyhole was recorded on videotape. The videosystem was used in an effort to discern pool flows. The welding operation was abruptly terminated to retain a "fossil" record of the keyhole. After the process was complete, the keyhole was characterized by its exit and entry hole diameters. The Oldeft system was used to acquire contour plots of sections of the crater, with the intent of assembling them into a three dimensional plot on the Viacom Image Analysis System. RTV-41 male replicas of the keyhole were made to help visualize the keyhole shape. The weld bead asymmetry, depth of undercut or grooving at the weld toe on the anterior surface, and sag on the posterior surface were characterized.

In the second program, production welding schedules were once again employed to produce keyhole welds on 0.375 inch Al 2219 plate. However, in addition to (and occasionally in place of) Aluminum 2319 filler wire, pure copper and Inconel 718 filler wires were used. Each of these surrogate filler materials has a melting point in excess of the aluminum alloy. (Al 2219, 660 deg. C; IN 718, 1500 deg.

C; Cu 1080 deg. C) The copper is quite soluble in the
aluminum alloy and forms a series of ordered compounds in
copper as well. The Inconel is not soluble in aluminum to an
appreciable extent. Despite the fact that the density of
these two materials is much greater than aluminum, it was
hoped that solidified globules of these materials would be
swept along in the pool currents, and that the distribution
of these globules could indicate pool flows. The shape of the
pool could be deduced by the addition of these fillers
immediately prior to arc termination. Longitudinal and
transverse sections of weld beads in the vicinity of the
terminal keyhole were made and sequentially polished to
determine pool flow patterns and pool shapes.

The third program was undertaken in order to to overcome
difficulties associated with the "in situ" examination of the
VPPA keyhole and molten weld pool. The observation of the
keyhole is limited on the anterior surface by the presence of
the bulky torch. The arc light and heat tend to obscure
observation of the keyhole from the posterior. Under optimal
conditions, only the surface of the pool is visible.

An analog was sought so that "in situ" examination of an
analog keyhole and pool could improve understanding of the
VPPA process. The following properties were sought:
            (1) Low melting point
            (2) Ease and saftey of handling
            (3) Verisimilitude to the hierarchy of forces in
                an actual weld
            (4) Transparency in the liquid state, so that
                volume flows could be directly observed, not
                inferred from surface flows.
Paraffin was found to satisfy the above desiderata fairly
well. The experimental apparatus is shown in Figures 6 and 7.
A soldering iron served as the source of heat for the analog
operation. Gas is heated in a coiled copper tube, wound
around the heating element and sealed by compound. A small
metal tip removed from a felt tip marker was press fit into
the output end of the copper coil in order to provide a
directed flow of heated inert gas. The delivery pressure was
regulated by supplying argon to the coil through the P2 flow
controller of the VPPA apparatus. The entire "torch" assembly
was mounted on a side beam that could be moved horizontally
to affect precise control of the standoff distance between
the assembly and the workpiece.

Plexiglas sheets (3"X5") were machined to various known
thicknesses, and slotted (2"X4") to serve as holding fixtures
for paraffin plates. After being taped down to Aluminum chill
plates these templates were filled with molten wax. The wax
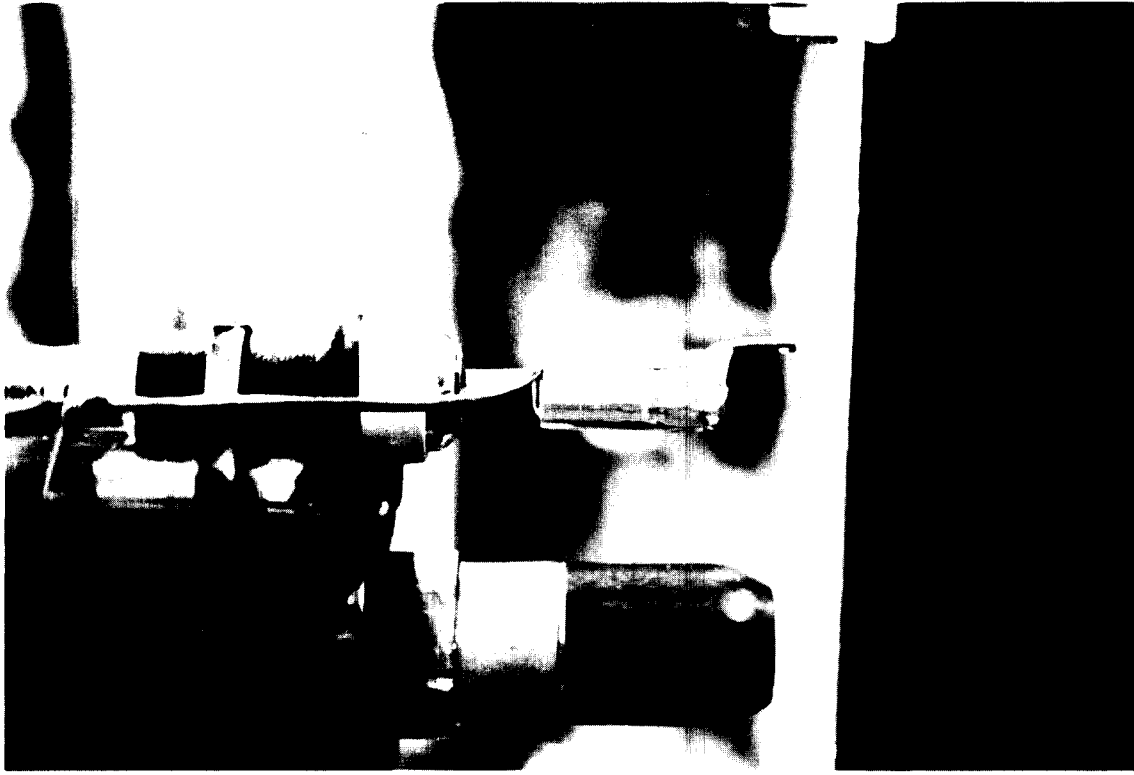
Figure 6. Analog Welding Apparatus
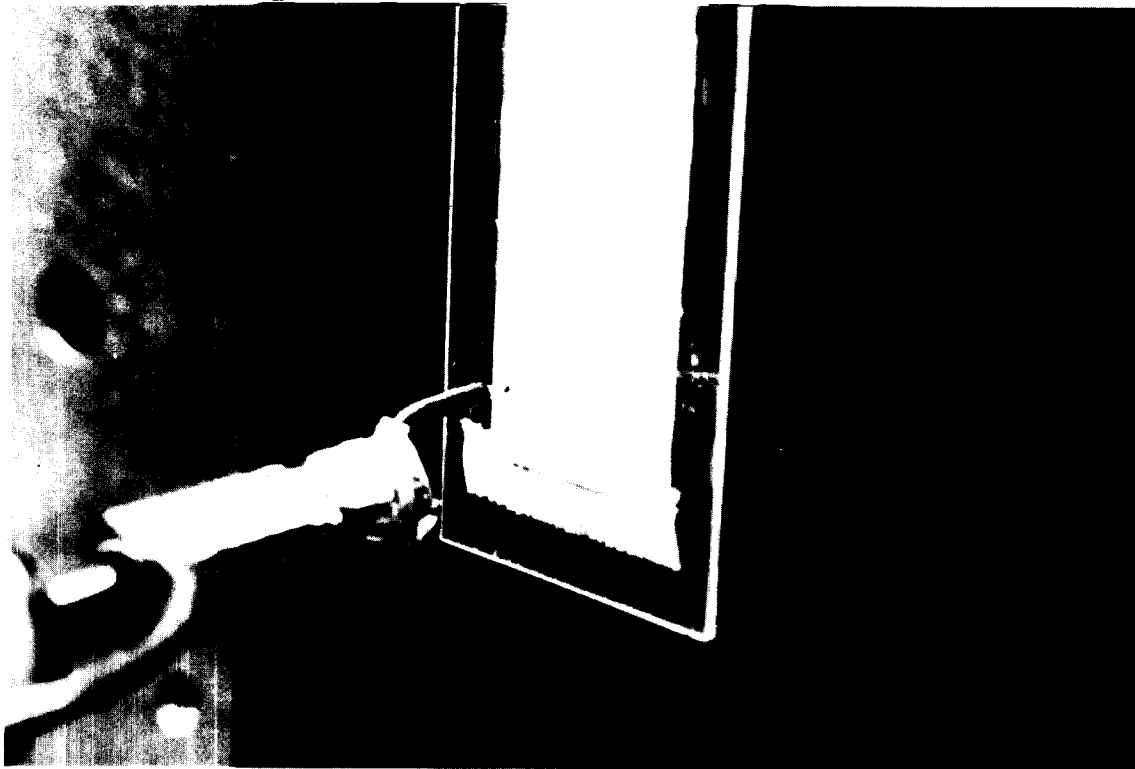
Figure 7. Wax Template and Welding Tip.

was allowed to harden, and was then shaved to uniform thickness. Small starter holes were drilled in the wax, and the template was placed on a vertical fixture capable of travel speeds up to one hundred inches per minute. The paraffin welding operation was recorded on videotape. The effects of changes in travel speed, standoff, gas flow rate, side angle and lag angle (torch lagging puddle) were examined and compared to similar changes in the VPPA process applied to Al 2219.

C-9

Results and Discussion

Chemical Additions

Table 1 lists the data collected for a variety of chemical additions to the weldment surface. The chemicals used are listed in the first column. (The letter B indicates that the chemical was placed on the posterior surface.) The second column lists the changes in plasma voltage caused by the presence of the chemical agent. The third indicates whether or not the agent produced a pool asymmetry. The next two columns list the depth of groove found at the deeper side of the bead, and the posterior reinforcement height respectively. The next two columns indicate the size of the entry and exit keyhole both without (WO) and with (WC) the addition. The next columns indicate the partial pressure of oxygen, listed as the base ten logarithm, of the pressure in atmospheres, expected in equilibrium with the oxides listed. Pressures are shown at temperatures of 1000, 1500, and 2000 degrees centigrade.

The partial pressures were estimated from available thermodynamic data. The free energy change associated with a reaction is

$$\Delta G = \Delta G_o + RT \ln K$$

$$\Delta G = \text{free energy of reaction}$$
$$\Delta G_c = \text{free energy of reaction at standard state}$$
$$K = \text{the equilibrium constant}$$

at equilibrium $\Delta G = 0$
and

$$\Delta G_o = -RT \ln K, \text{ or}$$
$$-\Delta G_c / RT = \ln K$$

for the reaction $\quad M + O_2 \quad MO_2$

K is given by $\quad \dfrac{a_{MO_2}}{a_M \, a_{O_2}} \quad a_i$ = the activity of species i

for pure solid elements or compounds, the activity is unity, thus

$$\Delta G_o / RT = \ln p \quad \text{and}$$
$$\exp(\Delta G_o / RT) = p$$

Many of the chemicals added had no discernible effect. Furthermore, otherwise active chemicals, when added to the posterior surface, produced no effect. Apparently there is little flow between the front and rear of the pool in Al 2219. Many chemicals altered the arc voltage, in each case raising it. The increase in voltage is not associated with increased standoff, but caused by electrical interactions in the plasma. A priori the voltage of the arc would be expected to fall in the presence of easily ionizable species. However the increase in the arc voltage can be explained if it is

Effects of Chemical Additions

Matl	ΔV	Asym	Groove	Sag	Entry WO/WC	Exit WO/WC	Temperature°C 1000	1500	2000
								$\lg_{10} p\ O_2$	
LiCl B	0	N	–	–	–	–			
MgSO B	0	N	–	–	–	–			
KBr B	0	N	–	–	–	–			
S	0	N	–	–	–	–			
Se	0	N	–	–	–	–			
Cu O	2.6	Y	0.12	0.22	.44/.5	.40/.54	-7	-3	-1
CaO	0	N	–	–	–	–	-41	-25	-17
TiO	0	N	–	–	–	–	-26	-15	-11
Al O	0	N	–	–	–	–	-38	-21	-15
Cr O	0	N	–	–	–	–	-20	-13	-8
CuSO	5.4	Y	BLOWTHROUGH		.44/.56	.34/.48			
CaSO	4.5	Y	BLOWTHROUGH		.40/.55	.36/.50			
CaCl	2.4	N	–	–	–	–			
CuCl	4.0	Y	0.09	0.16	.38/.46	.34/.39			
Fe O	4.5	Y	0.10	0.19	.40/.52	.36/.44	-5	-1	>1
MgSO	4.6	Y	BLOWTHROUGH		.44/.56	.38/.46			

Table 1 – Effects of Chemical Additions

associated with a small anode drop region that occupies the space above the anode spot to a height of several thousand angstroms. The presence of negatively charged species would be expected to increase the energy transfer to the pool at the anode spot. The most dramatic effects are caused by those species that contain oxygen. However, many of the oxides do not affect the welding process. This apparently anomalous behavior can be explained if the partial pressures of oxygen in contact with the oxide are reconciled to keyhole/pool behavior. The oxides CaO, TiO_2, Al_2O_3, and Cr_2O_3 have no effect on arc voltage or on pool shapewhen added to the keyhole environment. The oxides Cu_2O, and Fe_2O_3 foster an increase in plasma voltage, and lead to a pool asymmetry. Prior research has shown that oxygen at the 100 part per million level can drastically alter the amount of energy delivered to the pool. The maximum pool temperature can be estimated based on the activity (or lack thereof) of certain chemicals. Thus the maximum temperature expected would be between 1000 and 1200 degrees centigrade, and would be limited to that region directly beneath the anode spot. This contention is supported by the lack of incandescence associated with the trailing edge of the pool. Observations of the keyhole indicate that the anode spot is located on the leading edge of the pool, a region where the liquid film thickness is slight. This belief is supported by the observations that the efflux plasma is tilted downwards. The tilt is fostered by

(1) the shape of the keyhole channel
(2) an electromagnetic effect described by Maekler and Pfennder. (15,16)

Sulfates also produce dramatic effects. Oxygen present as water of hydration, and in the sulfate ion greatly increase the energy transfer to the pool. This results in an increase in the volume melted, and an imbalance in the forces that restore pool shape. Both molten volume and swept keyhole area increase as ΔV increases.

Pool Flow Markers

Filler additions facilitated identification of the steady state pool shape by distinctive etching characteristic. The flow was not well characterized by the distribution of filler rich regions. The addition of IN 718 as a continuosly fed filler caused a disruption in the pool and periodic blowthrough. This blowthrough is probably caused by the build up of heavy particles in the molten pool, the rupture of the retaining oxide film by shards of filler, or the weakening of oxide films in the presence of alloying elements.

Pool Analog

A pool analog was sought for the reasons listed previously. Table 2 lists the properties of paraffin and aluminum pertinent to a discussion of the model development, as well as a series of dimensionless numbers characterizing the two molten fluids. (17,18) As a basis for selection, a surface to weight force ratio was developed for an unsupported fluid contained in a cylinder of radius r and height h. The restoring force is simply $\gamma 2\pi r$

where γ is the surface tension.
The force caused by gravitational attraction is

$$\rho g \pi r^2 h$$

the ratio is therefore

$$2\gamma / \rho g r h$$

allowing r = h

$$2\gamma / \rho g r^2$$

this ratio becomes

The value of this parameter is similar for aluminum and paraffin. Rearranging the expression $r = \sqrt{\frac{2\gamma}{\rho g}}$

Thus the stable wax puddle will be somewhat smaller than the similar stable puddle in aluminum. (0.2 to 0.4 cm vis a vis 0.8cm)

The Marangoni number $\dfrac{\Delta T L_r (\partial \gamma / \partial T)}{\rho \alpha \nu}$

is indicative of the influence of surface tension driven flows in a material. It is the ratio of force produced by a thermally generated surface tension gradient, to forces resisting such flow. The large values of the Marangoni number observed for each fluid indicate that surface tension flows will exist in the molten pools.

The dynamic Bond number $\left(\dfrac{\partial \gamma}{\partial T}\right) \dfrac{1}{\Delta \rho \beta g L_r^3}$

is a ratio between the forces produced by surface tension, and those that arise from buoyancy effects. Again, the value listed indicates that surface tension driven flows will dominate the fluid in the keyhole region.

The final listed value is that for the Peclet number $\dfrac{U_r L_r}{\alpha}$
This number is indicative of the relative importance of convection and conduction in the weld pool. Convection dominates the transfer of heat in the molten metal. The pool morphology will be affected by any physical process that alters pool flow. In this respect VPPA keyhole welds are not unlike weld pools produced by other arc processes.

	ρ g/cm³	mp °C	$\beta\rho$ °C	β °C⁻¹	$\partial\gamma/\partial T$ d/cm²	C_p cal/kg°C	γ d/cm	k cal/cm s°C	μ cp
Aluminum	2.4	660	2450	114×10^{-6}	0.35	0.26	520	0.27	1.9
Parafin	0.9	55	--	12×10^{-6}	0.15	0.5	32	5×10^{-4}	1.0

	ALUMINUM	WAX	COMMMENTS
Surface to Weight Force Ratio			Design Parameter
	0.220	0.314	
Marangoni Number			Surface Tension Flows
	2.4×10^{5}	1.2×10^{7}	
Dynamic Bond Number			Surface Tension Flows/ Buoyancy Flows
	1.3×10^{3}	2.7×10^{4}	
Peclet Number			Relative importance of convection/conduction
	3.0×10^{2}	4.5×10^{2}	

Table 2 - Parameters of Comparison
Al and Paraffin

A procedure was developed to produce successful keyhole welds on paraffin of several different thicknesses. Figures 8 and 9 are photographs of wax keyhole welds made in paraffin 0.10 inches thick. Parameters for the welds depicted were chosen to intentionally produce asymmetric bead shapes (Fig. 8), and unstable beads (Fig. 9). The excessive undercut and asymmetry evident in the former case was generated by tilting the torch at a side angle of five degrees. It is interesting to note that one of the mechanisms known to produce undercut in actual VPPA weldments is arc misdirection. The instability in the latter case was caused by an increased lag angle (torch lags puddle). The effect is similar in VPPA welds when the "angle of attack is increased. The mass of molten fluid builds up until the restorative force of surface tension can no longer support the puddle. Interestingly parameters can also be chosen to produce a cutting action. In wax, or in aluminum this is accomplished by increasing the plasma pressure and by traveling faster. Furthermore, for a particular stable weld condition in paraffin increased standoff leads to a wider entrance hole and a diminished exit hole. This behavior is again analgous to the VPPA welding of aluminum.

A videotape of a keyhole weld in paraffin was made. Flow in the molten regions of the weld pool was readily apparent. Small solid paraffin fragments serve as excellent markers in a transparent pool. Two very strong vorticies (v = 35 cm/s) were observed near the head of the pool at the plate boundary. A strong general circulation was also noted in the center of the pool. These flows are consistent with those postulated based on Marangoni driven circulations. Figures 10 and 11, photographs of the paraffin keyhole, show very different pool shapes. The difference is caused simply by a change in travel speed. The shape of the weld pool in Figure 11 is similar to that found in VPPA welds studied during this investigation. The increase in pool length and the loss of elliptical shape is expected when the velocity increases, and has been observed in a variety of materials.
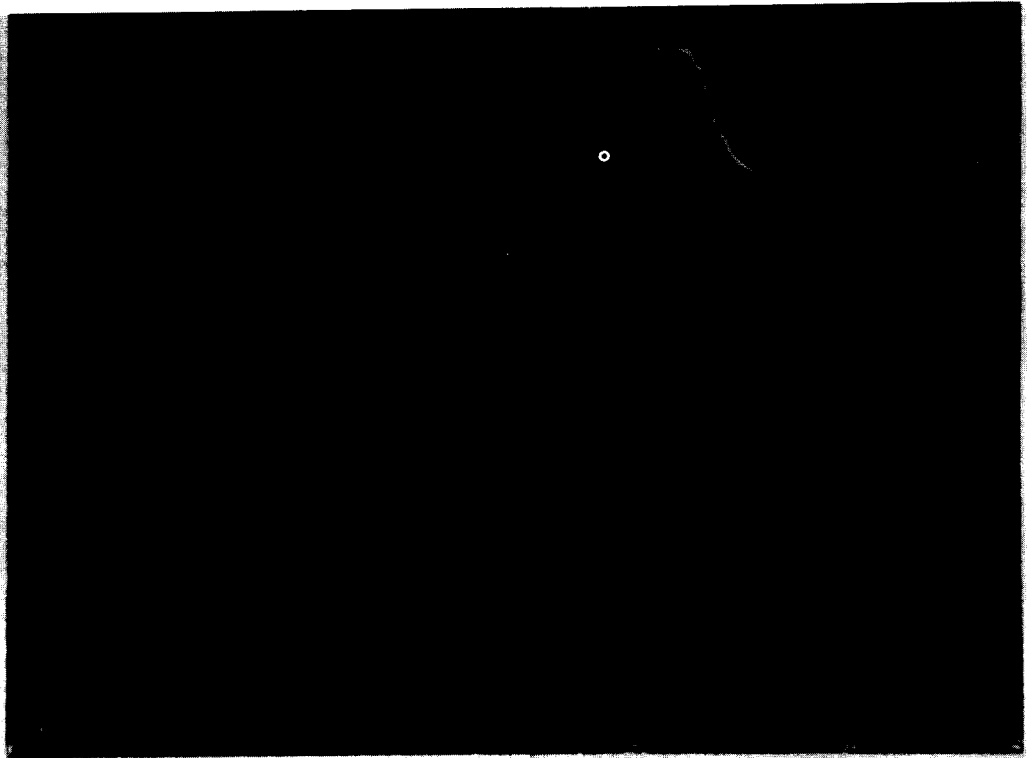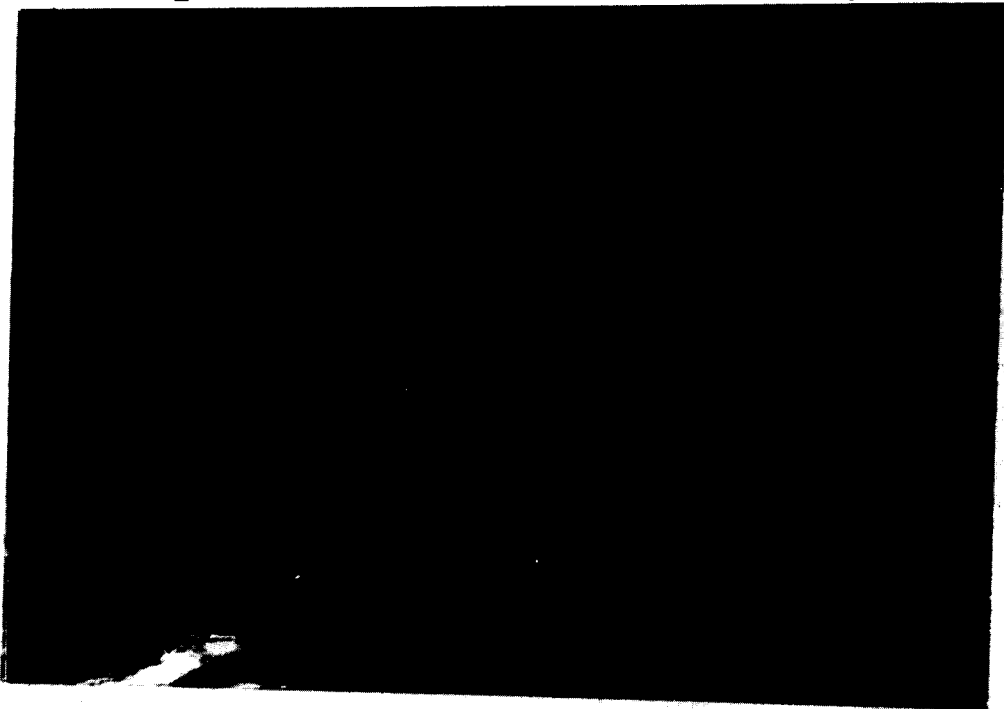
Figure 8. Analog weld in Paraffin, asymmetry.

Figure 9. Analog Weld in Paraffin, Unstable Bead.

Figure 10. Paraffin weld, high travel speed.

Figure 11. Paraffin weld, low travel speed

Conclusions

The results of this investigation indicate that:

1) The presence of oxygen in the keyhole regions of Al 2219 welds is damaging.

2) The critical level of oxygen is 10 atmospheres, a level easily developed by slight moisture contamination or by atmospheric permeation through gas hoses.

3) Oxygen interferes with the pool by altering processes at the anode. This increases the molten volume, and produces an instability caused by the increased weight of the pool. Volume considerations are primary, shifts in surface tension gradients caused by changing thermal gradients are secondary.

4) The presence of oxygen in the plasma increases the plasma voltage at fixed standoff. The voltage change is primarily associated with the anode drop region.

5) Marangoni surface tension driven flows dominate flow in the fluid surrounding the VPPA keyhole.

6) Pool flow in Al 2219 is direct Marangoni flow, no surface active elements produce flow reversals.

7) Flow in IN 718 and lithium added aluminum based alloys may be altered by the presence of surface active elements, and could be subject to flow reversals.

8) Chemical additions to the weld pool that increase the oxygen partial pressure in the keyhole region cause
   a) asymmetries that are similar to those produced by increased standoff and arc misdirection
   b) blow through in the pool if excessive melting and a weight imbalance occurs.

9) Chemical agents can be used to estimate pool surface temperature. The temperature in Al 2219 is 1000 to 1200 deg.C

10) The paraffin analog models a variety of VPPA effects.

11) The paraffin model allows convenient observation of bulk flows in the molten pool.

13) Solidified keyhole regions do not reflect the true shape of the keyhole "in process".

Suggestions for Future Work

1) Employ the wax analog to permit an extention of the understanding of fluid behavior in the keyhole. The analog can model a variety of VPPA parameters inexpensively.

2) Initiate a designed experimental program, in both Al 2219 and paraffin, to determine the relationship between the independent process variables and the dependent bead shape variables.

3) Examine the effects of shield gas additions on keyhole shape, deposit microstructure, and heat affected zone properties in Al 2219. This would improve understanding of the relationship between process and properties. Possible improvements in joint efficiency could lead to reduced flight weight.

4) Study Al 2519, and Al-Li alloys as available per the program outlined in (3). The program should be applied to IN 718 as well. The Al-Li alloys and IN 718 may behave quite differently than Al 2219. These alloys contain surface active elements that can cause surface tension driven flow **reversal** in the molten pool, and welding behavior unlike Al 2219. (This prediction is supported by the experience that MSFC personnel have had with IN718 and Al-Li) In the case of IN 718, the problem would be insidious, different heats of material could have grossly different flow characteristics.

5) Develop an impulse decanting system to allow exact determination of pool shape. This system would instantly remove over 99% of the molten pool and thus aid in the understanding of keyhole processes. The program would help to identify control variables for smart welding systems.

6) Develop vision systems to image the keyhole region, both front and rear. Employ the Viacom image analysis system to maximize the quantitative data gained in the effort. This would permit a clearer understanding of the metallurgy and physics of the keyhole region, while providing improved real time process control capability.

7) Use the arc/pool model developed by A. Nunes to model surface tension driven flow in VPPA welds, and in the analog. This would allow simplified quantitative modeling of puddle flows through use of quadrupoles. A study of the potential of this model for quantitative representation of puddle behavior could provide a useful too for analysis of and control of weld phenomena.

References

1) Metcalfe, J.C. and Quigley, M.B.,"Heat Transfer in Plasma Arc Welding", Welding Journal Research Supplement, 54, (3), 99s-103s, 1975.

2) Metcalfe, J.C. and Quigley, M.B., "Keyhole Stability in Plasma Arc Welding", Welding Journal Research Supplement, 54, (11), 401s-404s, 1975.

3) Tomsic, M.J. and Jackson, C.E., "Energy Distribution in Keyhole Mode Plasma Arc Welds", Welding Journal Research Supplement, 53, (3), 109s-115s, 1974.

4) Shaw, C.B., "Diagnostic Study of the Plasma Arc", Welding Journal Research Supplement, 58, (4), 121s-125s, 1980.

5) Andrews, J.G., Atthey, D.R. and Byatt-Smith, J.G., "Weld Pool Sag", J. Fluid Mechanics, 100, (4), 785-800, 1980.

6) Okamoto,I.,Omori, A., and Kihara, H.,"Role of Surface Tension in Fusion Welding, Pt.2", Transactions of the Japanese Welding Research Institute, 12, (1), 1983.

7) Woods, R.A. and Milner, P.R., "Motion in the Weld Pool in Arc Welding", Welding Journal Research Supplement, 50, (4), 1971.

8) Andrews, J.G. and Craine, R.E., "Fluid Flow in a Hemisphere Induced by a Distributed Source of Current", J. Fluid Mechanics, 84, (2), 1978.

9) Atthey, D.R., "A Mathematical Model for Fluid Flow in a Weld at High Currents", J. Fluid Mechanics, 98, (4), 1980.

10) Mills, M.S., "Fundamental Mechanisms of Penetration in GTA Welding", Welding Journal Research Supplement, 58, (1), 1979.

11) Landau, L. and Lifshitz, E., Fluid Mechanics, Addison Wesley, 1959, p252.

12) Levitch, V.G., Physiochemical Hydrodynamics, Prentice Hall, 1962, p388.

13) Kou, S., and Konevesky, T., "Welding Thin Plates of Aluminum", Welding Journal Research Supplement, 61, (6), 1972

14) Oreper, G.M. and Eagar, T.W., "Convection in Arc Weld Pools", Welding Journal Research Supplement, 62, (11), 1983.

15) Pfender, E. and Eckert, E.R., "Plasma Energy Transfer to Surface With and Without Electric Current", Welding Journal Research Supplement, 46, (10), 471s-480s, 1967.

16) Maecker, H., Z. Physizk., 141, 198, 1955.

17) CRC Handbook of Chemistry and Physics, 1975.

18) Physical Properties of Liquid Metals, Oak Ridge National Laboratory, 1959.